ELECTROCHEMICAL DISSOLUTION OF MIXED OXIDES OF Mn AND Fe: THE RELATIONSHIP BETWEEN PHASE COMPOSITION AND REACTIVITY

TOMÁŠ GRYGAR, SNEZHANA BAKARDJIEVA, PETR BEZDIČKA, PETR VORM

Institute of Inorganic Chemistry AS CR, 250 68 Řež, Czech Republic
E-mail: grygar@iic.cas.cz

Submitted September 11, 2000; accepted December 15, 2000.

Reductive dissolution of mixed oxides of Mn and Fe was studied by voltammetry of microparticles in acetate buffer at pH 4.4. The following four series were synthesized: (1) C-Mn_2O_3 to α-Fe_2O_3, (2) $LiMn_2O_4$ to $LiFe_5O_8$, (3) $CaMnO_3$ through $Ca_3(Mn,Fe)_3O_{8+x}$ to $CaFe_2O_5$, and (4) almost amorphous MnO_x to FeOOH. The ranges of isostructural solid solutions were identified by XRD analysis. The following solid solutions with continuous change of both structure and dissolution reactivity were found: the bixbyite C-$(Fe,Mn)_2O_3$ part in series (1), the whole spinel series (2), and O-deficient perovskite $Ca_3(Mn,Fe)_3O_{8+x}$ in the middle of (3). The stability range of $Ca_3(Mn,Fe)_3O_{8+x}$ depends on the calcination temperature. Mn-doped hematite α-$(Fe,Mn)_2O_3$ with Fe/(Fe+Mn)=0.9 is not reductively dissolved before hydrogen evolution. The reductive dissolution of $CaMnO_3$ part of (3) significantly depends on the calcination temperature. Mn(IV) in the series (4) is most easily reductively dissolved, and only the series (4) behaves like a physical mixture of two phases with two separate reaction steps corresponding to reductive dissolution of Mn(IV) and Fe(III). Voltammetric peak potentials of C-$(Fe,Mn)_2O_3$ and $LiMn_2O_4$ - $LiFe_5O_8$ are very sensitive to Fe content, whereas the lattice parameters are negligibly affected by Fe amount in the former case.

INTRODUCTION

Redox dissolution is an important degradation reaction of transition metal oxides, which contain metal ions with more possible valences. For example the attack of $Cr^{III,IV}$, $Mn^{III,IV}$, and Fe^{III} oxides by oxidizing or reducing agents is usually the only way to their dissolution in aqueous medium. In hydrometallurgy the dissolution is an intentional part of Fe and Mn ore processing [1, 2], and it is used for decontamination of steel surfaces in water systems of nuclear reactors [3]. On the other hand in the case of metal-oxide electrodes for electrolysis, batteries, pigments and heterogeneous catalysts the dissolution can be fatal. The actual dissolution reactivity of metal oxides can hence be of a great practical importance and should be a part of the tests of materials exposed to redox species in solutions. $Mn^{III,IV}$ and Fe^{III} can be reductively dissolved via reactions

$$Fe_2O_3(s) + 2\ e^- + 6\ H^+ \rightarrow 2\ Fe^{2+}(aq) + 3\ H_2O$$

$$MnO_2(s) + 2\ e^- + 4\ H^+ \rightarrow Mn^{2+}(aq) + 2\ H_2O$$

Reductive dissolution of both Fe^{III} oxides [4] and $Mn^{III,IV}$ oxides [5] proceed quantitatively in acidic solution and the dissolution have certain phase selectivity. Fe and Mn form several mixed oxides, reductive dissolution of which has not yet been described in literature. Substitution of Fe in α-Fe_2O_3, α-FeOOH and $MeFe_2O_4$ by another trivalent metal ion, such as Al and Cr, suppresses their reactivity toward reductive dissolution [3, 6 - 10]. The resistance of Ni, Fe, Cr-oxides to their dissolution in aqueous solutions is responsible for the protective efficiency of passivating oxide films on austenitic steels but adversely complicates cleaning the oxidized steel surfaces [3], and so dissolution of Fe, Cr oxides has been relatively well described. However, no systematic study has been published dealing with the influence of Mn-substitution in a wide range of Fe/Mn ratio. Another reason for the interest in reactivity of mixed oxides of Fe and Mn is that incorporation of Fe has been tested to improve the properties of $LiMn_2O_4$ battery electrode materials [11, 12]. However, the influence of substitution on the reactivity of metal oxides is usually a very complex problem, which is rarely systematically studied in electrochemical literature unless it brings substantial improvement of the utility values of battery electrodes.

We synthesized and electrochemically dissolved mixed oxides of the following series: C-Mn_2O_3 (bixbyite) – α-Fe_2O_3 (hematite); $LiMn_2O_4$ – $LiFe_5O_8$ (spinels) [13]; and $CaMnO_3$ (perovskite) – $Ca_3(Fe,Mn)_3O_{8+x}$ (O-deficient perovskite) – $CaFeO_{2.5}$ (brownmillerite). These oxides are present in ores, they

Paper presented at the conference Solid State Chemistry 2000, Prague, September 3 - 8, 2000.

have been tested or used as anodes for electrolysis, electrode materials for power sources, catalysts, and magnetic materials. The knowledge about their redox dissolution can hence have a certain practical importance. The dissolution reactivity of Fe, Mn oxides can be conveniently followed by voltammetry of microparticles [4, 5, 8, 9, 14]. Besides less important influence of particle size [4] the reactivity of oxide powders should depend mainly on the oxide structure and on Fe/(Fe+Mn) ratio. This study is a part of our attempt to find a relationship between reactivity toward electrochemical dissolution and structure and crystallinity of transition metal oxides.

EXPERIMENTAL PART

The mixed oxides of the bixbyite-hematite series, Ca,Mn-perovskite – Ca,Fe-brownillerite series, Cr and Co doped Ca,Fe-brownmillerite, and Li, Fe, Mn-spinels of series C were prepared by thermal decomposition of metal nitrates and citric acid. Appropriate amount of 1 M solutions of metal nitrates were mixed in a beaker and citric acid in the molar ratio of citric acid and nitrates 1 to 1.5 was added and dissolved in ultrasonic bath and under heating. The clear solution was evaporated on hot plate, the dry residue was carbonized at about 400 °C, and then calcined at the final temperature on air. Final temperature was 850 °C for hematite-bixbyite and for spinel series C, and 1000 or 1150 °C for perovskite-brownmillerite series. The samples of $CaMnO_3$ were calcined at temperatures between 850 and 1150 °C. The spinel solid solutions of series S were obtained as described elsewhere [13], i.e. by calcination of Fe,Mn-oxide precursors with Li_2CO_3 at 600 to 850 °C. For a comparison, poorly crystalline to amorphous oxides of Fe and Mn were prepared by fast oxidative hydrolysis of Fe^{2+} and Mn^{2+} by alkaline solution of hydrogen peroxide to demonstrate the behavior of an almost amorphous system. The resulting solids were dried at 80°C on air. The synthesis was adopted according to ref. [15].

Elemental composition of oxides was determined by atomic absorption (Fe,Mn) and emission spectroscopy (Li, Ca). Redox state was determined by iodometry (in the absence of Fe in oxide) or permanganometry after dissolution in ferrous sulfate solutions (in the presence of Fe in oxide).

Phase composition of the phases was checked by X-ray diffraction using Siemens D5005, CuKα radiation, 40 kV, 30 mA, diffracted beam monochromator. Qualitative analysis was done with Bede ZDS for Windows, quantitative analysis and refinement of the cell parameters with PowderCell for Windows. Structure refinement was performed with FullProf based on Rietveld analysis.

The dissolution reaction was followed using voltammetry of microparticles [14] in solutions of appropriate acidity (acetate buffer, $pH = 4.4$, or solution of $NaClO_4$ and $HClO_4$, $pH = 2$). Measurements were performed with potentiostat μAutolab controlled by GPES 4.4 program by EcoChemie, Utrecht, the Netherlands. Samples were deposited by intensive rubbing of a pile of sample on filter paper with a paraffin-impregnated graphite working electrode. Saturated calomel electrode (SCE) was used as reference, and Pt-plate as counterelectrode. Linear sweep voltammetry at 1 mV/s scan rate was used to obtain well-defined peak-shaped voltammetric curves. The scanning started at open circuit potential and continued to negative potentials. The current is proportional to the actual dissolution rate through

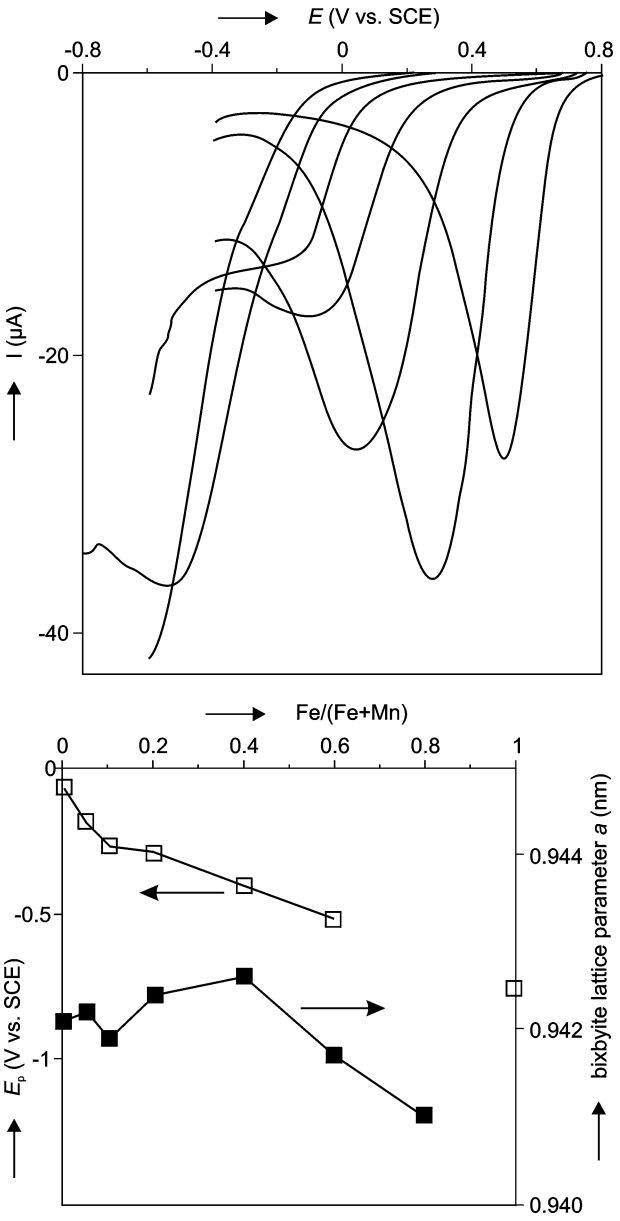

Figure 1. Voltammetric curves of Mn_2O_3-Fe_2O_3 solid solutions and the dependence of peak potentials and lattice parameter a of Fe-bixbyite on Fe/(Fe+Mn). The numbers at voltammetric curves are Fe/(Fe+Mn) in molar %. Mn doped hematite did not yield dissolution peak under conditions applied.

Table 1. C-Mn_2O_3-α-Fe_2O_3 series: peak potentials of reductive dissolution in acetate buffer at scan rate 1 mV/s, and lattice parameters obtained by XRD data processing with PowderCell.

Fe/(Fe+Mn)	E_P (V vs. SCE)	C-Mn_2O_3				α-Fe_2O_3	
		a (nm)	*b* (nm)	*c* (nm)	%	*a* (nm)	*c* (nm)
0	-0.07	0.9421	0.9406	0.9408	100		
0.05	-0.19	0.9422	0.9405	0.9414	100		
0.1	-0.27	0.9419	0.9413	0.9412	100		
0.2	-0.29	0.9424	0.9407	0.9411	100		
0.4	-0.405	0.9426	0.9411	0.9408	100		
0.6	-0.52	0.9417	0.9402	0.9410	100		
0.8	wave	0.9410	0.9404	0.9411	43	0.5036	1.3736
0.9	wave					0.5036	1.3739
1	-0.76					0.5035	1.3736

Faraday's law. More details about reductive dissolution of metal oxides were given in our previous papers [4, 5, 8, 9].

RESULTS AND DISCUSSION

C-Mn_2O_3 – α-Fe_2O_3

Intermediate members of this series were Fe-doped bixbyite and Mn-doped hematite. Bixbyite is built of very distorted octahedra in a cubic oxygen sublattice [16], whereas hematite has hexagonal oxygen sublattice and metal ions occur in regular octahedral holes. Hence the series is not continuous, and the miscibility gap is at Fe/(Fe+Mn) ~ 0.3 according to the XRD analysis using PowderCell. The lattice parameters of bixbyite are almost independent on Fe/(Fe+Mn).

The dissolution peaks of Fe-substituted bixbyite in acetate buffer continuously shifted toward more negative potentials up to Fe/(Fe+Mn) = 0.6 (figure 1 and table 1). The continuous dependence of the peak potential of Fe-substituted bixbyite reductive dissolution intimates the behavior of ideal solid solutions of two electroactive species. When Mn-substituted hematite arose beside Fe-substituted bixbyite, the voltammetric peak changed to a wave. Single-phase Mn-doped hematite with Mn/(Fe+Mn) = 0.1 was not electrochemically reducible before hydrogen evolution. The same level of Cr substitution also causes passivation of hematite [9, 10]. Pure hematite is again completely reductively dissolved before hydrogen evolution in acid solution [4, 17, 18].

As follows from data in table 1 and figure 1, the actual Fe/(Fe+Mn) valence has more significant influence on the oxide reactivity toward reductive dissolution than to their lattice parameters obtained by XRD.

$LiMn_2O_4$ – $LiFe_5O_8$

All the members of the series are cubic spinels without any discontinuities in the structure with changing Fe/(Fe+Mn) except for non-ideal behavior of Li distribution between octahedral and tetrahedral positions [19, 20]. Although the Mn valence varies between III and IV, the charge equilibrium is reached by changing Li/(Fe+Mn) ratio and oxygen deficiency is not created as in the perovskite case discussed hereafter. Accordingly all the members of the spinel series were reductively dissolved with the potential of the corresponding voltammetric peaks shifting continuously to more negative values with the growing content of Fe. The influence of Fe/(Fe+Mn) ratio is comparable to those in the series bixbyite-hematite, but in the spinel series even the Fe rich members are electrochemically dissolved. The peak potential of the spinels is not significantly affected by Mn valence. It may be caused by the reaction mechanism of the reductive dissolution of majority of Mn^{IV}-containing oxides, that starts with Mn^{IV} to Mn^{III} reduction in the solid state, and continues by the reduction of Mn^{III} to Mn^{II} that is finally chemically dissolved. The reduction steps of Mn^{IV} and Mn^{III} are overlapped at the *pH* chosen (acetate buffer, *pH* = 4.4) [5], and so a single peak of reductive dissolution is observed. More detailed report about electrochemical reactivity of Li, Fe, Mn-spinels is currently prepared for publication [21].

$CaMnO_3$ – $Ca_3(Fe,Mn)_3O_{8+x}$ – $CaFeO_{2.5}$: XRD study

This series was studied first by Coats and McMillan [22] who recognized three phases in this system. Although Coats and McMillan used relatively high synthesis temperature (1350 °C), they found a major fraction of Mn in tetravalent state in the whole series. The system was then studied systematically as it attracted attention of structural chemists [23, 24]. The quantitative analysis of XRD patterns of this series was done using three structural models. The regions of the occurrence of these three species are given in table 2 together with the results of refining lattice parameters of these phases. Lattice parameters of all three phases changed continuously with changing Fe/(Fe+Mn) following the Veggard rule.

Table 2: The perovskite-brownmillerite series: peak potentials of reductive dissolution in acetate buffer at scan rate 1 mV/s, and lattice parameters. Structural models of $Ca_2Fe_2O_5$, $Ca_3Fe_2TiO_8$, and $CaMnO_3$ were used for processing XRD data by PowderCell or Fullprof.

Fe/(Fe+Mn)	T (°C)	E_P(V vs. SCE)	$Ca_2(Fe,Mn)_2O_5$			$Ca_3(Fe, Mn)_3O_{8+x}$			
			a (nm)	b (nm)	c (nm)	a (nm)	b (nm)	c (nm)	%
0.975	1150	no peak	0.5421	1.4786	0.5589				
0.95	1150	no peak	0.5417	1.4809	0.5583				
0.90	1150	no peak	0.5409	1.4855	0.5569				
0.85	1150	no peak	0.5400	1.4896	0.5552				
0.80	1150	wave	0.5397	1.4928	0.5536	0.5479	1.1149	0.5362	50
0.75	1150	wave	0.5388	1.4918	0.5513	0.5477	1.1144	0.5359	43
0.70	1150	-0.18	0.5387	1.4933	0.5515	0.5528	1.1133	0.5392	100
0.65	1150	-0.17	0.5383	1.4931	0.5515	0.5472	1.1149	0.5358	100
0.78	1000	-0.24				0.5473	1.1145	0.5360	100
0.60	1150	-0.11	$CaMnO_3$			0.5469	1.1168	0.5352	100
0.58	1000	-0.11				0.5462	1.1177	0.5349	100
0.55	1150	-0.11	a (nm)	b (nm)	c (nm)	0.5447	1.1167	0.5353	79
0.525	1150	-0.08				0.5436	1.1191	0.5339	51
0.49	1050	-0.10	0.5325	0.7520	0.5325	0.5414	1.1176	0.5358	13
0.37	1000	-0.07	0.5318	0.7488	0.5314				
0.40	1150	-0.15	0.5316	0.7507	0.5311				
0.30	1150	-0.19	0.5307	0.7508	0.5311				
0.20	1150	-0.26	0.5301	0.7484	0.5287				
0.10	1150	-0.17	0.5281	0.7451	0.5274				
0.00	1150	-0.16	0.5279	0.7451	0.5266				

The series begins with orthorhombically distorted perovskite $CaMn^{IV}O_3$, space group Pnma (ICSD 35218) [25]. For fitting a part of Mn was replaced by Fe.

For the intermediate Ca,Fe,Mn-phase we adopted model of orthorhombic phases $Ca_3Fe_{1.8}Mn_{1.2}O_8$, space group Pcm21 (ICSD 203100) [24]. The structure is derived from perovskite structure by regular alterations of the planes of octahedra and tetrahedra with periodicity OOT along b-axis [24]. The samples were single-phase at $0.45 < Fe/(Fe+Mn) < 0.6$ after calcination at 1150 °C, that is similar to the range $0.53 < Fe/(Fe+Mn) < 0.6$ found for this phase by Nguyen et al. [23]. At 1000 °C the stability range of this phase is even wider, i.e. at least $0.37 < Fe/(Fe+Mn) < 0.78$ (see table 2). At 850 °C, two-phase samples were obtained containing the oxygen deficient perovskite and $CaMnO_3$. The samples synthesized at 1150 °C contained all Mn in tetravalent state according to chemical analysis. Consequently the stoichiometry of the sample with $Fe/(Fe+Mn) = 0.49$ can be written as $Ca_3Fe_{1.47}Mn_{1.53}O_{8.26}$. The oxygen content is than higher than that reported by Rodríguez-Carvajal et al. [24] ($Ca_3Fe_{1.8}Mn_{1.2}O_{8.055}$). The difference is much bigger if compared to $Ca_2FeMnO_{5.06}$ supposedly obtained by Nakahara et al. [26], who obtained their sample by air calcination at 1150 - 1200 °C and identified its structure as brownmillerite $Ca_2Fe_2O_5$. Both oxygen content and structure of the phase reported by Nakahara et al. [26] are in significant contradiction to the published data and our results. Mn valence close to four was also found in $CaMnO_3$ calcined at temperatures close to 1000°C on air [27].

Fe rich members with $Fe/(Fe+Mn) > 0.7$ at 1150 °C were identified as orthorhombic $Ca_2Fe_2O_5$, space group Pnma (ICSD 15059) [28], and their lattice parameters were obtained by replacement of a part of Fe in 4c positions by Mn.

$CaMnO_3$ – $Ca_3(Fe,Mn)_3O_{8+x}$ – $CaFeO_{2.5}$: Reductive dissolution

The reductive dissolution of $CaMnO_3$ was already found to be different than those found for other Mn^{IV} oxides [5], as the reaction mechanism involves probably one-electron rate-determining step. In this work we further observed a significant shift of the peak potential of the reductive dissolution of individual $CaMnO_3$ samples calcined at different temperatures, that is demonstrated in figure 2. The higher the calcination temperature the more negative was the peak potential of reductive dissolution. This peak potential of $CaMnO_3$ calcined at 850 °C (further denoted as low temperature samples) was similar to that of $LiMn_2O_4$, and their XRD patterns have features of poorly crystalline solids with broadened diffraction lines. The more negative dissolution peak potential of the samples calcined at above 1000 °C (high-temperature samples) resembled rather Fe^{III} oxides and Mn^{III} containing bixbyite, although according to chemical analysis Mn is mainly tetravalent. The relationship between synthesis

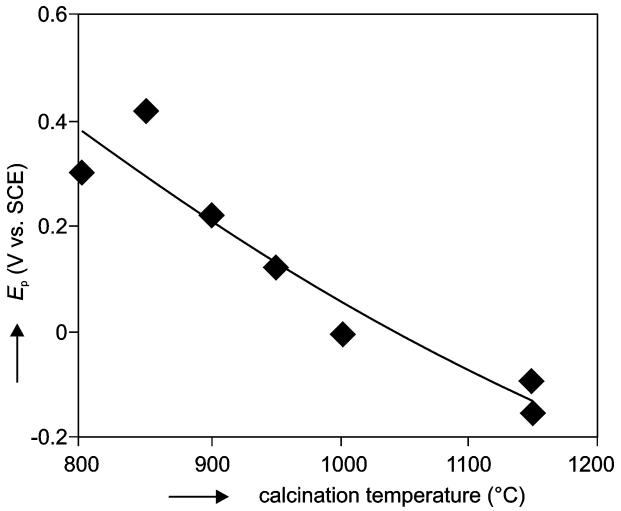

Figure 2. The dependence of peak reductive dissolution potentials of $CaMnO_3$ on their calcination temperature.

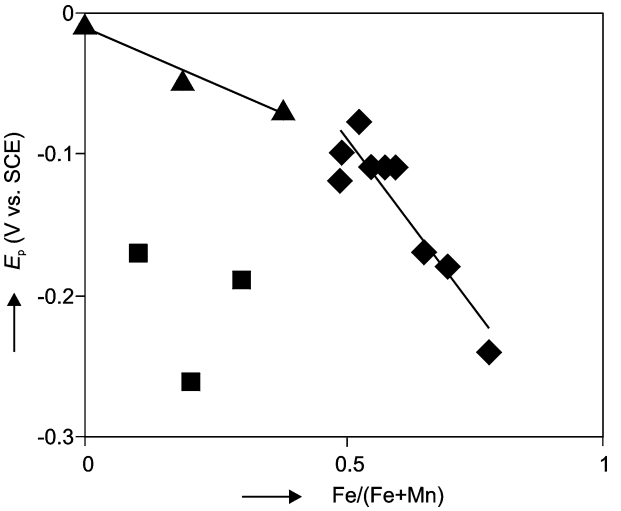

Figure 3. The dependence of peak potentials and phase composition of Ca, Fe, Mn-oxides on Fe/(Fe+Mn). Brownmillerite is not reductively dissolved under conditions applied. Denotation of experimental points: perovskite isostructural with $CaMnO_3$ obtained by calcination at 1000°C (▲) and at 1150°C (■), and O-deficient perovskites $Ca_3(Fe,Mn)_3O_{8+x}$ (◆).

conditions and electrochemical reducibility was also reported by Morimoto et al. [27], who tested suitability of rare-earth doped $CaMnO_{3-y}$ as battery materials. Probably due to the sensitivity of the phase to the synthesis conditions, the voltammetric peak potentials of $Ca(Fe,Mn)O_3$ cannot be directly related to the Fe/(Fe+Mn) ratio.

With increasing Fe content, an oxygen deficient perovskite isostrucural with $Ca_3Fe_{1.8}Mn_{1.2}O_8$ was formed. This phase was electrochemically reductively dissolved at potentials comparable to high-temperature samples of $CaMnO_3$ (figure 3). Voltammmetric peak potential E_P of the single-phase samples statistically significantly depended on their Fe/(Fe+Mn) ratio (r^2 = 0.84 for n = 9), and on the contrary to $CaMnO_3$ the peak potentials were not substantially different after calcination at 1000 or 1150 °C.

The brownmillerite-type samples formed at Fe/(Fe+Mn) > 0.75 were not electrochemically reductively dissolved before hydrogen evolution reaction neither in acetate buffer nor in solution of $HClO_4$. As the content of brownmillerite phase increased at Fe/(Fe+Mn) > 0.7 after calcination at 1150 °C, the voltammetric peak of reductive dissolution of O-deficient perovskite $Ca_3(Fe,Mn)_3O_{8+x}$ vanished without a significant shift of the peak potential of the residual oxygen-deficient perovskite. Neither Cr- nor Co-doped $Ca_2Fe_2O_5$ were not reductively dissolved. Brownillerite $Ca_2Fe_2O_5$ is hence another Fe^{III} oxide which is not reductively dissolved in aqueous acidic environment. Such inertness was recently also reported for undoped $LaFeO_3$ [29].

Poorly crystalline phases MnO_x-$Fe(O,OH)_y$

XRD analysis did not clearly identify the phase composition of the mixed samples of this series (table 3). Formation of birnessite from Mn^{2+} salt is in accordance with the original report on this synthesis [15]. As to dissolution reactivity the mixture of almost amorphous Mn and Fe oxides behaved as a physical mixture of the oxide components with two peaks characterizing the individual members of series (table 3, figure 4). All samples were reductively dissolved in acetate buffer and in solution of $HClO_4$. There was practically no continuous change of the peak potentials in the series. The composition of samples resembled the deep-sea manganese nodules, which processing is based

Table 3: Poorly crystalline series.

Fe/(Fe+Mn)	XRD	E_P1 (V vs. SCE)	E_P2 (V vs. SCE)
0.0	birnessite (PDF 43-1456)	0.53	-
0.25	birnessite + line at d = 0.46 nm	0.5	wave
0.5	line at d = 0.10 nm	0.5	wave
0.75	no diffraction lines	0.46	-0.1
1.0	no diffraction lines	no	-0.15

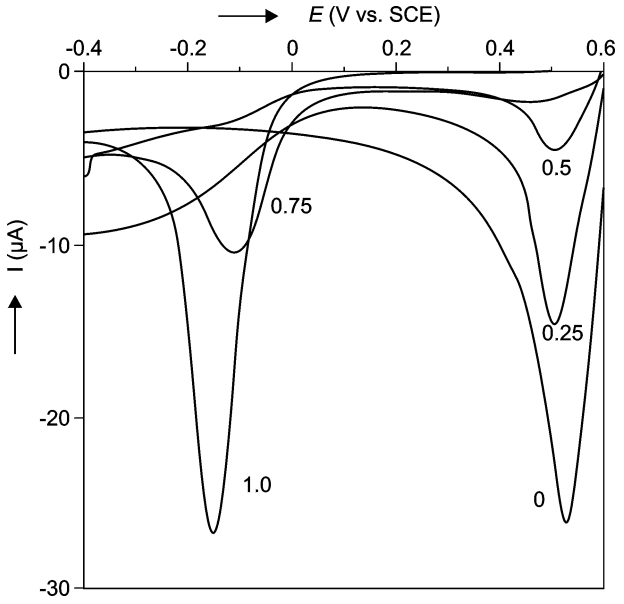

Figure 4. Voltammograms of poorly crystalline Fe, Mn oxides obtained by fast oxidative hydrolysis. The numbers at voltammetric curves denote actual Fe/(Fe+Mn).

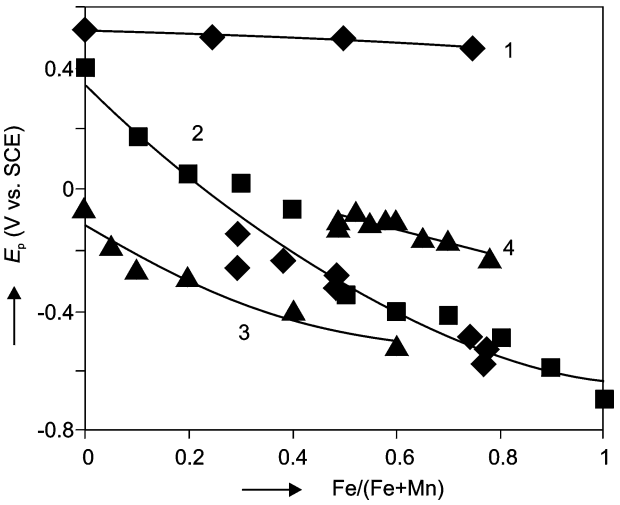

Figure 5. Comparison of peak potentials of dissolution vs. Fe/(Fe+Mn). Poorly crystalline Fe, Mn oxides (1), Li, Fe, Mn spinels (2), C-Mn_2O_3 - α-Fe_2O_3 (3) and $CaMnO_3$-$Ca_3(Fe,Mn)_3O_{8+x}$ series (4). In the dependence for spinels, ■ denote samples of series S and ◆ those of series C.

on their relative easy reductive dissolution in aqueous solutions [2]. On the contrary to the well-defined mixed oxides of Fe and Mn described above, the poorly crystalline samples are easily reductively dissolved and no passivation due to the substitution was observed.

CONCLUSION

The reactivity of the studied Fe, Mn-oxide series toward reductive dissolution depended significantly on the individual phase composition and Fe/(Fe+Mn) content. Generally the potential required for the reductive dissolution in a given series shifted to more negative values with increasing Fe content if the series is a well-defined solid solutions. The miscibilty gaps as in the Mn_2O_3-Fe_2O_3 series or $CaMnO_3$-$Ca_3(Fe,Mn)_3O_{8+x}$ causes abrupt changes in the E_P plots against Fe/(Fe+Mn) or disappearance of voltammetric peaks due to inertness of a new phase. The three single-phase series studied, bixbyite $(Fe,Mn)_2O_3$, spinel $(Li,Fe,Mn)_3O_4$, and oxygen deficient perovskite $Ca_3(Fe,Mn)_3O_{8+x}$ hence yield three lines of E_P vs. Fe content with different slopes and abscissas in figure 5. It is noteworthy that the reductive dissolution potential generally depends on Mn valence, as the peak potentials of these oxides decrease at a given Fe/(Fe+Mn) from O-deficient perovskite containing exclusively tetravalent Mn through spinels with Mn valence between III and IV to bixbyite with exclusively trivalent Mn. From analytical point of view the sensitivity of reductive peak potential E_P to Fe content in bixbyite is much bigger than that of lattice parameters that could possibly find application for electroanalysis of bixbytite samples of unknown Fe content.

Besides this systematic behavior we observed two uncommon phenomena. The first one is the reductive dissolution resistance of pure, Co, Cr, and Mn-doped brownmillerite $Ca_2Fe_2O_5$, and Mn-doped hematite α-Fe_2O_3. The inertness of Mn-doped hematite to reductive dissolution resembles passivity of Cr-doped hematite toward chemical [3] and electrochemical [9, 10] reductive dissolution. This passivity is surprising in the case of Mn^{III} doping especially with respect to the significant reactivity of Mn_2O_3 toward reductive dissolution. The second unusual observation was a dependence of reductive dissolution reactivity of $CaMnO_3$ on the calcination temperature.

Acknowledgement

The work was supported by Grant Agency of Academy of Sciences, project no. S4032004.

Authors thank to Prof. Emilia Wolska from A. Mickiewicz Univeristy, Poznaň, Poland for kindly providing the Li,Fe,Mn-spinels, series S, and to Jan Framberk, Insitute of Inorganic Chemistry, Řež, Czech Republic, for elemental analysis.

References

1. Das S.C., Sahoo P.K., Rao P.K.: Hydrometallurgy *8*, 35 (1982).
2. Acharya R., Ghosh M.K., Anand S., Das R.P.: Hydrometallurgy *53*, 169 (1999).
3. Joseph S., Venkateswaran G., Moorthy P.N.: J. Nucl. Sci.Technol. *36*, 798 (1999).

4. Grygar T.: Coll.Czech.Chem.Commun. *60*, 261 (1995).
5. Bakardjieva S.,Bezdička P., Grygar T.: J. Solid State Electrochem. *4,* 306 (2000).
6. Sellers R.M., Williams W.J.: Faraday Discuss. Chem. Soc. *77*, 265 (1984).
7. Torrent J., Schwertmann U., Baron V.: Clay Miner. *22*, 329 (1987).
8. Grygar T.: J. Solid State Electrochem. *1***,** 77 (1997).
9. Grygar T., Bezdička P., Caspary E.G.: J. Electrochem. Soc. *146,* 3234 (1999).
10. Schmuki P., Virtanen S., Isaacs H.S., Ryan M.P., Davenport AJ., Böhni H., Stenberg T.: J. Electrochem. Soc. *45,* 791 (1998).
11. Song M.Y., Ahn D.S., Kang S.G., Chang S,H.: Solid State Ionics *111*, 237 (1998).
12. Song M.Y., Ahn D.S.: Solid State Ionics *111*, 245 (1998)
13. Wolska E., Stempin K., Krasnovska-Hobbs O.: Solid State Ionics *101-103*, 527 (1997).
14. Scholz F., Meyer B.: *Voltammetry of Solid Microparticles Immobilized on Electrode Surfaces*, in *Electroanalytical Chemistry, A Series of Advances*, Ed. by Bard A J., Rubinstein A, *Vol. 20*, p. 1, Marcel Dekker, Inc 1998.
15. Feng Q., Yanagisawa K., Yamasaki N.: J. Mater. Sci. Letters *16*, 110 (1997).
16. Rao C.N.R., Raveau B.: *Transition Metal Oxides, Structure, Properties, and Synthesis of Ceramic Oxides*, 2nd edition, Wiley VCH, New York - Chichester - Weinheim - Brisbane - Singapore - Toronto 1998.
17. Lecuire J.-M.: J. Electroanal. Chem. *66*, 195 (1975).
18. Mouhandess M.T., Chassagneux F., Vittori O.: J. Electroanal. Chem. *131*, 367 (1982).
19. Blasse G.: Philips Res. Repts. *20*, 528 (1965).
20. Wolska E., Piszora P., Stempin K., Catlow C.R.A: J. Alloys Comp. *286,* 203 (1999).
21. Grygar P., Bezdička P., Piszora P., Wolska E.: J. Solid State Electrochem. - in print.
22. Coates R.V., McMillan J.W.: J. Appl. Chem.-USSR *14*, 346 (1964).
23. Nguyen N., Calage Y., Varret F., Ferey G., Caignaert V., Hervieu M., Raveau B.: J. Solid State Chem. *53*, 398 (1984).
24. J. Rodríguez-Carvajal, M. Vallet Regi, J. M. Gonzalez Calbet: Mater. Res. Bull. *24*, 423 (1989).
25. K. R. Poeppelmeier, M. E. Leonowicz, J. C. Scanlon, J. M. Longo, W. B. Yelon: J. Solid State Chem. *45*, 71 (1982).
26. Nakahara Y., Kato S., Sugai M., Ohshima Y., Makino K.: Mater. Letters *30*, 163 (1997).
27. Morimoto H., Kamata M., Esaka T.: J. Electrochem. Soc. *143*, 567 (1966).
28. Berggren J.: Acta Chem. Scand. *25*, 3616 (1971).
29. Grygar T.: J. Solid State Electrochem. *3,* 412 (1999).

ELEKTROCHEMICKÉ ROZPOUŠTĚNÍ SMĚSNÝCH OXIDŮ Mn A Fe: VZTAH MEZI FÁZOVÝM SLOŽENÍM A REAKTIVITOU

TOMÁŠ GRYGAR, SNEZHANA BAKARDJIEVA, PETR BEZDIČKA, PETR VORM

Ústav anorganické chemie AV ČR, 250 68 Řež

Reduktivní rozpouštění směsných oxidů Mn a Fe bylo studováno voltametrií mikročástic v acetátovém pufru při *pH* 4. Byly připraveny čtyři řady vzorků: (1) C-Mn_2O_3 až α-Fe_2O_3, (2) $LiMn_2O_4$ až $LiFe_5O_8$, (3) $CaMnO_3$ přes $Ca_3(Mn,Fe)_3O_{8+x}$ až $CaFe_2O_5$, a (4) takřka amorfní MnO_x až FeOOH. Rozmezí isostrukturních tuhých roztoků bylo nalezeno RTG práškovou difrakční analýzou. Byly nalezeny následující tuhé roztoky se spojitou změnou struktury a rozpouštěcí reaktivity: bixbyitová C-$(Fe,Mn)_2O_3$ část řady (1), celá spinelová řada (2), a O-deficitní perovskit $Ca_3(Mn,Fe)_3O_{8+x}$ ve středu řady (3). Rozsah stability $Ca_3(Mn,Fe)_3O_{8+x}$ záleží na kalcinační teplotě. Mn-dopovaný hematit α-$(Fe,Mn)_2O_3$ s Fe/(Fe+Mn)=0.9 se nerozpouští před vylučováním vodíku. Reduktivní rozpouštění $CaMnO_3$ části řady (3) významně závisí na kalcinační teplotě. Mn(IV) v sérii (4) se rozpouští nejsnadněji a jen řada (4) se chová jako fyzikální směs dvou fází s odlišnými rozpouštěcími stupni odpovídajícími reduktivnímu rozpouštění Mn(IV) a Fe(III). Potenciály voltametrických píků C-$(Fe,Mn)_2O_3$ a $LiMn_2O_4$ - $LiFe_5O_8$ jsou velmi citlivé k obsahu Fe, zatímco mřížkové konstanty jsou v prvním případě jen zanedbatelně ovlivněny obsahem Fe.